Vortex Dynamics Associated with the Impact of a Cylinder with a Wall

Lionel SCHOUVEILER[‡], Mark C. THOMPSON[⋆], Thomas LEWEKE[‡], Kerry HOURIGAN[⋆]

[‡] *Institut de Recherche sur les Phénomènes Hors Équilibre (IRPHE), CNRS/Universités Aix-Marseille, 49 rue Joliot-Curie, B.P. 146, F-13384 Marseille Cedex 13, France*
[⋆] *Fluids Laboratory for Aeronautical and Industrial Research (FLAIR), Department of Mechanical Engineering, Monash University, Victoria 3800, Australia*

Abstract. The flow resulting from the oblique collision without rebound of a circular cylinder with wall in a still viscous fluid is investigated both computationally and experimentally. We focus on the dynamics of the different vortex systems that form during such a motion and on their dependance on the impact angle. For this purpose, dye visualizations and numerical simulations using a spectral-element method are performed.

Key words: cylinder impact, vortex dynamics, DNS, spectral-element method, flow visualization.

1. Introduction

A solid body colliding with a solid surface is a common situation in everyday life, involving complex energy exchanges. We focus here on the hydrodynamic effects resulting from such a collision. Their understanding is of interest for industrial applications, such as heat exchangers using fluidized-bed technology, where the collisions of particles with surfaces create strong currents allowing to enhance heat exchanges due to the resulting forced convection. A study like the present one, of the impact of an individual particle can also help understand particle-laden flows. Moreover, when the collision occurs on a dusty surface, the resulting flow gives rise to dust resuspension (see, *e.g.*, [1]), an issue of importance to environmental and climate studies.

2. Methodology

The flow resulting from the normal or oblique collision without rebound of a circular cylinder (diameter D) on a wall in a still viscous fluid is investigated. For this purpose, the cylinder is impulsively started from rest, travels a distance L through the fluid at a constant velocity U towards a wall, then stops at the moment of contact with the wall. The parameters of this configuration (see Fig. 1) are the non-dimensional travel distance L/D, the Reynolds number $Re = UD/\nu$, where ν the fluid's kinematic viscosity, and the impact angle α, *i.e.*, the angle between the body trajectory and the normal to the wall. In the present paper we mainly focus on the dependance of the vortex dynamics on the impact angle α. For this

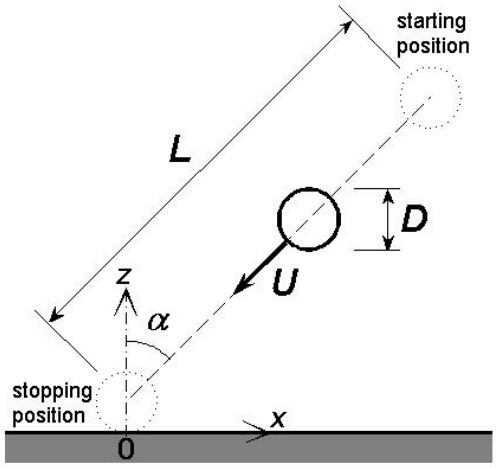

Figure 1. Problem definition and parameters.

purpose visualizations are performed for 5 values of α, namely 0°, corresponding to the normal impact, 21°, 33°, 47° and 62°. Experiments were performed at a Reynolds number $Re = 200$, for which the flow stays two-dimensional, except near the cylinder ends. This Reynolds number is above the critical value of around 50 for the onset of vortex shedding behind the cylinder. Because we wish to limit the present investigation to stationary initial states, with two symmetrical vortices of opposite sign attached behind the cylinder, the approaching distance L/D is chosen short enough to avoid the development of vortex shedding, but large enough for the development of well-defined vortices. These conditions are met for the distance $L/D = 4$ considered here.

2.1. Numerical method

The numerical approach for investigating the hydrodynamics associated with the impact of a particle on a wall is based on the spectral-element method incorporating a deforming mesh. More details on the method can be found in Thompson *et al.* [2].

2.2. Experimental details

Experiments are conducted in a 600 mm high glass tank with a square horizontal cross-section of 500×500 mm^2, filled with water. An aluminium cylinder of length 368 mm and diameter $D = 15.91$ mm is suspended horizontally using two inelastic threads (see Fig. 2). The threads are attached to a computer controlled stepper motor, allowing to lower the body at a specified velocity U, and to impulsively stop the cylinder motion at the position of contact with the wall. An inclined wall is placed at the bottom of the tank. It consists in a plate of plexiglas attached to a second plate (using a swivel articulation), itself placed at the bottom of the

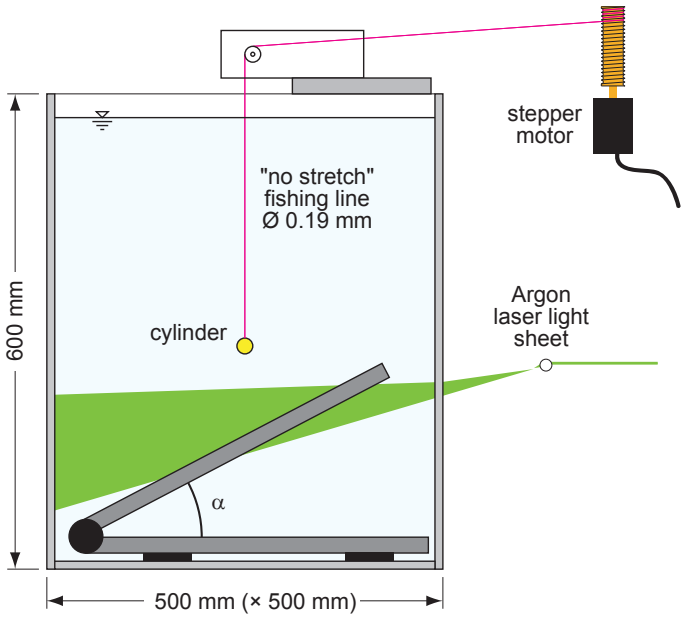

Figure 2. Experimental setup.

tankThis allows for a continuous variation of the inclination angle. The cylinder axis is perpendicular to the wall slope in such a way that the contact between the cylinder and the wall after impact is a line perpendicular to the wall slope.
For the visualizations, the cylinder is coated with a solution of green fluorescent dye prior to lowering it into the water. Dye patterns created by the flow entrainment are illuminated by a vertical light sheet perpendicular to the cylinder axis and passing by its center. An argon laser beam is spread out by a cylindrical lens for generating the light sheet. Visualizations are recorded with a digital video camera operating at 25 frames per second and aligned with the cylinder axis. The movies are then analyzed frame by frame to extract the vortex trajectories. We use the coordinate system shown in Fig. 1, and time t is non-dimensionalized using the advection time scale: $\tau = t/(D/U)$. The origin $\tau = 0$ corresponds to the instant of impact.

3. Results

3.1. Normal collision

Figure 3 shows, for a normal impact ($\alpha = 0$) at $Re = 200$, dye visualizations at the instant of the impact ($\tau = 0$) and three different times after the impact corresponding to $\tau = 2.1$, 4.9 and 15.1, as well as the corresponding evolution of the vorticity field deduced from the numerical predictions.
While the cylinder approaches wall, the dye is entrained into the two longitudinal vortices that form in its wake, as can be seen at the instant of the impact $\tau = 0$. After the impact, these primary vortices continue to travel towards the wall because of the inertia, thus going round the cylinder. Then they impact the wall and are convected away from the cylinder. This motion induces secondary vorticity on the cylinder surface that rolls up to form a secondary longitudinal vortex of opposite

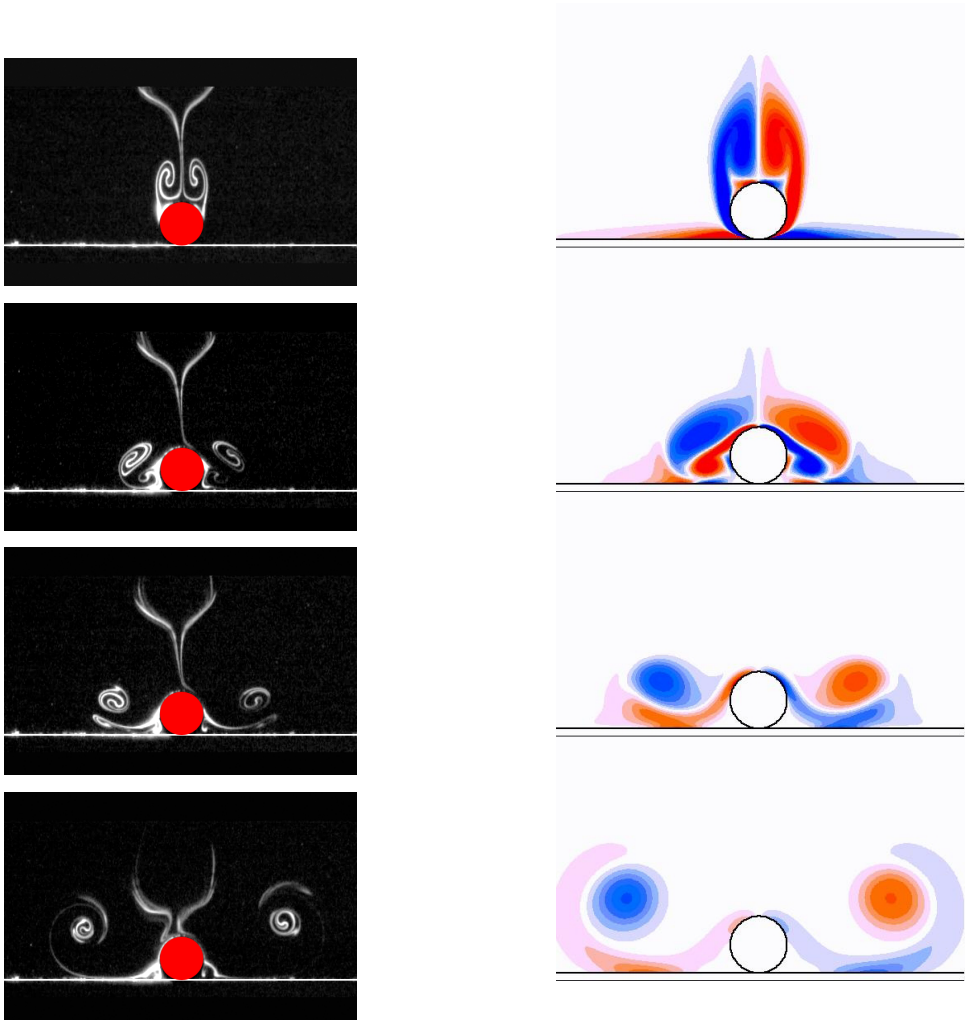

Figure 3. Flow visualizations (left) and simulations (right) of the cylinder impact for $Re = 200$, $L = 4D$ *and* $\alpha = 0$*;* $\tau = 0, 2.1, 4.9, 15.1$ *from top to bottom.*

sign on each side of the cylinder ($\tau = 2.1$). Simulations show another source of secondary vorticity of same sign in the viscous boundary layer at the wall, that can not be exhibited by the visualizations because the dye is on the sphere surface. Secondary vorticity encircles the primary vortex when time increases.

Both dye visualizations and numerical simulations show that the planar symmetry with respect to the plane $x = 0$ is preserved during the normal impact for this value of the Reynolds number. Experimental trajectories of the primary vortex centers and of the centers of the secondary vortices that are induced at the sphere surface are plotted in Fig. 4. Experimental vortex centers are defined as being the center of the dye spiral that appear on the visualizations.

Centers of the secondary vortices can be followed for a short time between $\tau = 0.7$ and $\tau = 2.8$ because of the fast diffusion of the vorticity. In contrast with secondary vortices, it is possible to follow the primary vorticity centers for a long time. Their trajectories are nevertheless plotted for $\tau = 0$ to 20.3 only, because it has been

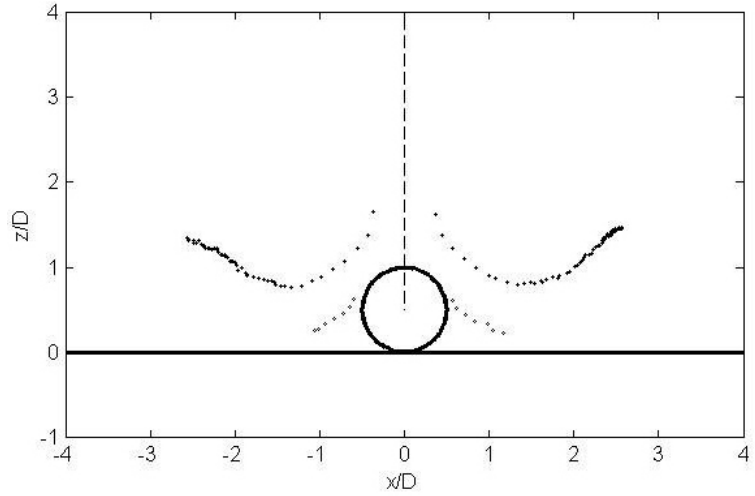

Figure 4. Trajectories of vortex centers for $Re = 200$*;* $L = 4D$*,* $\alpha = 0$*. Primary wake vortices (•) and secondary vortices from sphere surface (∘).*

previously shown (Thompson *et al.* [3]) that, due to the large difference between the diffusivities of dye and vorticity, the dye centers are a good markers for the maximum of the vorticity for a limited time only.

Fig. 4 shows that primary wake vortices are advected radially outwards with an additional vertical "rebound" component due to the secondary vorticity.

3.2. Oblique collision

For investigating the effect of the impact angle α between the normal to the wall and the cylinder trajectory, experiments have been performed for 4 values of α, namely $21°, 33°, 47° and 62°$, in addition of the case of the normal impact $\alpha = 0$ described in the previous section. Figure 5 compares dye visualizations and vorticity fields as deduced from the numerical simulations for the intermediate angle $\alpha = 33°$ and Fig. 6 for the maximum angle investigated $\alpha = 62°$.

We first note on Figs. 5 and 6 that for non-normal impacts, the planar symmetry is not preserved even at the initial instant $\tau = 0$.

On the far side of the impact line ($x < 0$) the wake vortex and the secondary one combine together into a pair of vortices of opposite sign. Such a dipole structure has a self-induced velocity, which is responsible for its ejection, as seen on Figs. 5 and 6. The trajectories of the centers of these two vortices appear curved towards the primary vortex (see Fig. 7), because this vortex is stronger than the secondary one. Comparison of Figs. 7(a) to (d) show that the radius of curvature tends to increases with α, because the relative difference in strength of the two vortices tends to diminish with α. On the other side of the contact line, the primary vortex travels on smaller circles because the circulation of the secondary vortex is much lower than the one of the primary vortex.

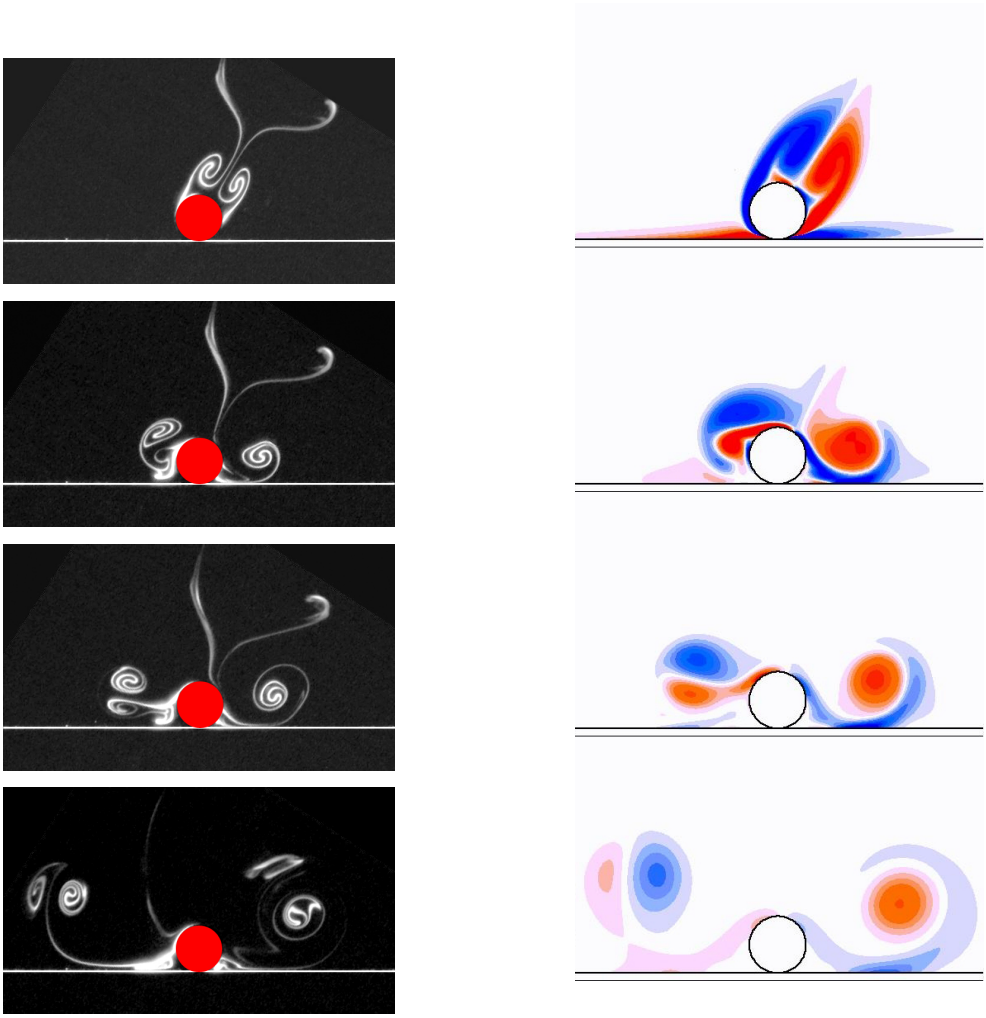

Figure 5. Flow visualizations (left) and simulations (right) of the cylinder impact for $Re = 200$, $L = 4D$ *and* $\alpha = 33°$; $\tau = 0, 2.1, 4.9, 15.1$ *from top to bottom.*

4. Conclusion

Numerical simulations and experimental flow visualizations have been performed for investigating the hydrodynamics of a cylinder impacting a wall, these two approaches show good agreement. Non-normal collisions give rise to strong vortex dipoles that are advected over long distance from the impact area. This flow leads to an increase of the mass transfer that can result in an enhancement of mixing and heat transfer at the wall.

References

[1] Eames I., Dalziel S.B., *Dust resuspension by the flow around an impacting sphere*, J. Fluid Mech. 403, 305-328, **2000**.

[2] Thompson M.C., Hourigan K., Cheung A., Leweke T., *Hydrodynamics of a particle impact on a wall*, Appl. Math. Modelling 30, 1356-1369, **2006**.

[3] Thompson M.C., Leweke T., Hourigan K., *Sphere-wall collision: vortex dynamics and stability*, J. Fluid Mech. 575, 121-148, **2007**.

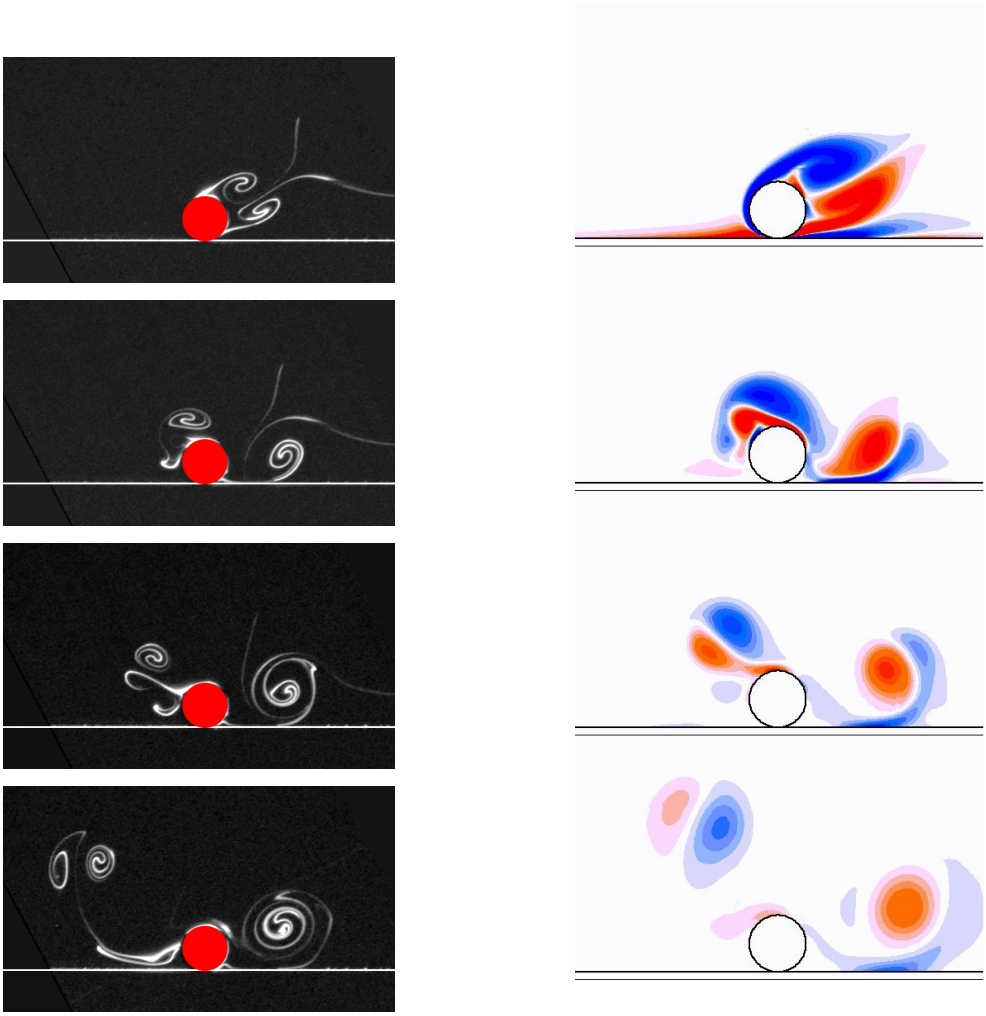

Figure 6. Flow visualizations (left) and simulations (right) of the cylinder impact for $Re = 200$, $L = 4D$ *and* $\alpha = 62°$*;* $\tau = 0, 2.1, 4.9, 15.1$ *from top to bottom.*

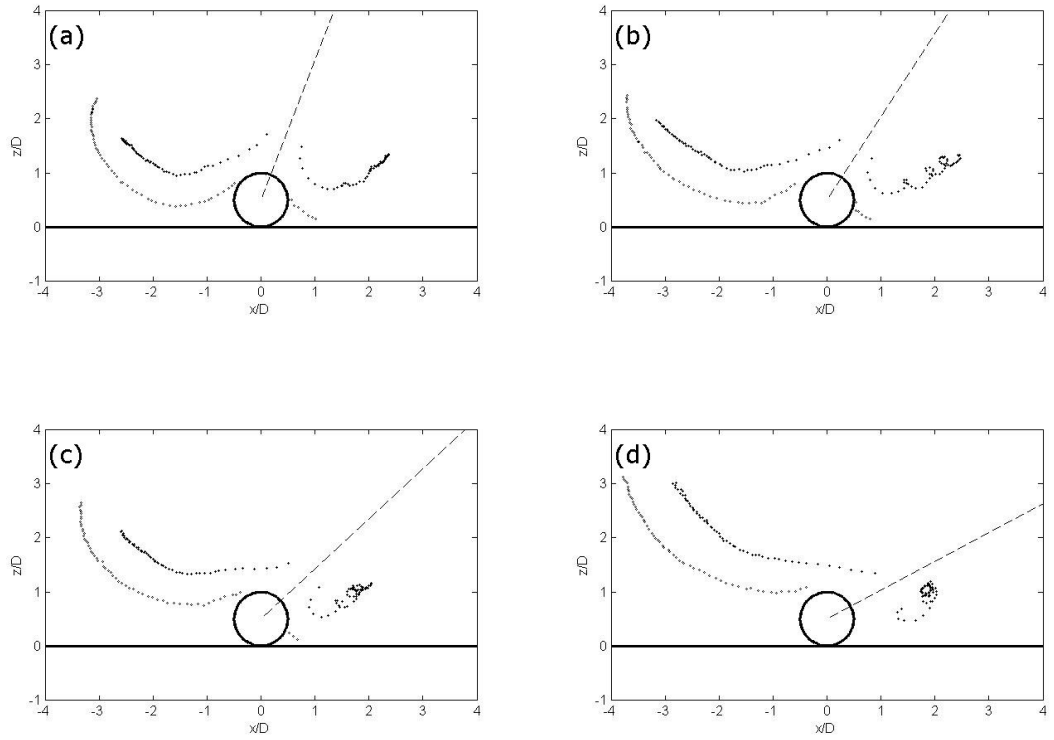

Figure 7. Trajectories of vortex centers for $Re = 200$; $L = 4D$. (a) $\alpha = 21°$, (b) $\alpha = 33°$, (c) $\alpha = 47°$, (d) $\alpha = 62°$. Primary wake vortices (•) and secondary vortices from sphere surface (○).